TRAVELLING WAVE AND STANDING WAVE SINGLE CELL HIGH GRADIENT TESTS *

V.A. Dolgashev, S.G. Tantawi, C.D. Nantista, SLAC, Menlo Park, CA, 94025, USA

Y. Higashi, T. Higo, KEK, Tsukuba, Ibaraki 305, Japan

INTRODUCTION

Accelerating gradient is one of the crucial parameters affecting the design, construction and cost of next-generation linear accelerators. The present Next Linear Collider (NLC) / Global Linear Collider (GLC) designs specifies unloaded accelerating gradient of 65 MV/m at 11.4 GHz [1]. This is almost three times the present operating gradient of the S-band SLAC linac. The major obstacle to higher gradient is rf breakdown.

RF breakdown limits working power and produces irreversible surface damage in high power rf components and rf sources. For a given rf frequency, the maximum working gradient depends on the rf circuit, structure geometry and material. It is also a function of the input power, pulse width, and surface electric and magnetic fields. Here we define working gradient as a gradient with very low breakdown rate — less then one breakdown in 2×10^6 rf pulses.

The complexity of rf breakdown phenomena and the absence of a proven theory for it make it difficult to apply experimental results on breakdown limit from one rf structure to another. For example, working gradients in specialized small cavities are usually much higher than in high power waveguides and practical accelerating structures. To date, dozens of full-scale travelling wave (TW) structures [1, 2] and standing wave (SW) structures [3] have been tested at SLAC in an effort to produce accelerating structures that satisfy NLC/GLC requirements on gradient and breakdown rate. The requirements were met mainly by reducing length of a structure. To reach the same gradient while keeping average iris size, the power fed into a structure had to be reduced. Many questions about the physics of rf breakdown remain unanswered. The experiments described in this paper are designed to study the breakdown phenomena. They allow economical testing of structures with different cell geometries, materials and preparation techniques with short turn around time. The requirements were met mainly by reducing the power fed into a structure. To reach the same gradient while keeping average iris size, structure length had to be reduced. Many questions about the physics of rf breakdown remain unanswered.

MOTIVATION

The shape of the cell is one of the parameters that determines the high power performance of an accelerating structure. To study the effect of cell shape on the rf breakdown behavior of a TW structure is difficult because the geometry of the cells varies along its length and rf power decays toward the end of the structure. Here we refer to 11.424 GHz, near-constant-gradient TW structures developed for the NLC [2].

In order to study the effect of cell shape alone, we will perform an experiment with *single cell TW* structures. The idea is to build a structure that in only one cell mimics the fields near the input of a full-scale TW structure and has high electric and magnetic fields only in that cell, not in matching elements or *couplers* that transform the TE_{10} mode of rectangular waveguide into the "accelerating" circular TM_{01} mode. Another feature of the setup is the couplers, or mode launchers, which can be connected to the single cell structure with rf-compatible circular waveguide vacuum flanges. The flanges allow re-use of the same mode launchers for different structures, significantly reducing the cost of the experiments and allowing fast turn-around between tests of different structures.

We emphasize the difference between our proposed tests and earlier experiments with single cell structures [4]: the power available for breakdown and the field configuration in the single TW cell are similar to the power and fields at the beginning of the full TW accelerating structure. This was not the case in earlier experiments, which were done mostly with standing wave structures. We note that available rf power was shown in experiments [2] to have an effect on the breakdown limit in full TW structures.

Since breakdown behavior in TW structures and SW structures is different [3, 5], to study this difference and effect of SW cell shape on breakdown, we will perform *single cell SW* experiments. These will employ one of the mode launchers to feed rf power into a SW structure. Fields in the middle cell of the SW structure are similar to fields of a large-aperture SW structure already tested at high power (structure SW20a565 [3]). Fields in the other two cells are designed to be at most one half of the middle cell fields, so breakdowns will likely occur in the middle cell.

We note that shapes and field distributions in both single cell TW and single cell SW structures are identical to shapes and fields of full-length structures. We speculate that this similarity will allow us to predict the behavior of practical structures from the tests. We note another advantage of the single cell structures: small geometry allows better diagnostics of breakdown events and makes possible detailed 3D simulation of breakdown processes observed in the experiments.

SETUP

The TW single cell setup consists of two mode launchers with a TW structure in between. The SW single cell setup consists of one mode launcher and a SW structure. Mode

---

launchers and standing wave structures have have vacuum viewports to detect visible light and high frequency rf signals generated by breakdown events.

Mode Launcher

The mode launcher transforms the TE_{10} mode of WR90 rectangular waveguide into the TM_{01} mode in circular waveguide with a diameter of 0.900 inch (2.286 cm). It is designed as a single unit with rectangular and circular rf vacuum flanges and a vacuum viewport. A cutaway view of the mode launcher is shown in Fig. 1.
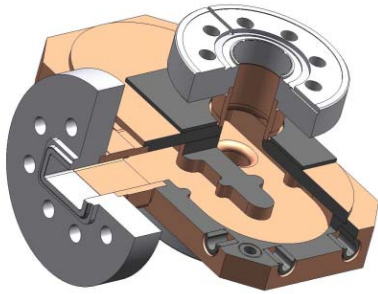

Figure 1: Cutaway view of the mode launcher.

Power in the WR90 input is split with a matched T, then symmetrically fed into the perpendicular circular waveguide. In the circular waveguide at 11.424 GHz only two modes are supported: TE_{11} and TM_{01}. With symmetric feeding, the TE_{11} mode is suppressed, and even with imperfect feeding symmetry it is poorly coupled to the rectangular TE_{10} mode (due to the field orientation). With only TM_{01} excited, a simple matching element in WR90 — a thick inductive iris — completes this launcher. Results of cold test measurement for the mode launchers are presented in [6]. Four mode launchers were built and successfully cold tested. Although the mode launcher itself was not yet tested at high power, nine couplers for travelling wave structures, based on the design, have been successfully used in the high-gradient structure program at SLAC [6].

Travelling Wave Structures

In the single cell TW setup, fields of the TM_{01} mode are first generated by the mode launcher, then transformed by a matching cell into fields of a periodic structure travelling wave (in one cell), then transformed through another matching cell back to the TM_{01} waveguide mode, to be extracted by the second mode launcher. The dimensions of the single cell are chosen to be the same as an initial cell of TW structure known as T53VG3. This is a disk-loaded waveguide with initial group velocity 3% speed of light and 120° phase advance per cell. The iris radius for the cell is 3.88 mm, the iris thickness 1.66 mm, the cell radius 10.641 mm, and the cell length 8.747 mm.

To create the travelling wave in one cell, we first match the 0.9 inch circular waveguide into a semi-infinite disk loaded waveguide using one matching cell. The matching process is described in detail in [6]. Then we make a structure with only one cell between two matching cells. Fields in this single cell structure are shown in Fig. 2. To illustrate
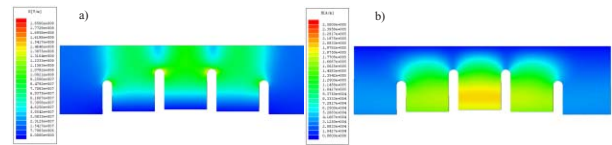

Figure 2: Amplitude of electric (a) and magnetic (b) fields in single cell TW structure for 40 MW of input power.

the properties of the structure we show calculated reflection of the TM_{01} mode from a structure made of the same matching cells and one, four, and 10 cells on Fig. 3. This
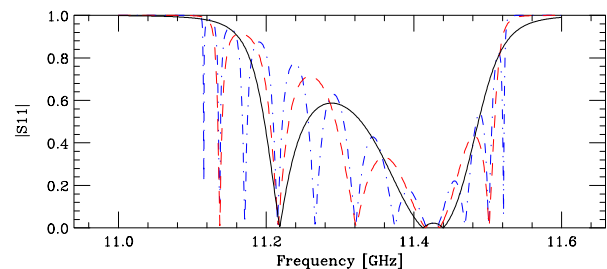

Figure 3: Reflection from a setup with different numbers of cells sandwiched between two matching cells: single cell (solid curve), 4 cells (dashed), and 10 cells (dot-dashed).

graph clearly shows that the match at working frequency, 11.424 GHz, is independent of the number of cells, *i.e.* the matching cell creates fields with space harmonic content close to that of the travelling wave in periodic disk-loaded waveguide.

A total of five TW structures were built for the test, including one structure that has iris tips made of molybdenum. All of them were successfully cold tested. In Fig. 4, we show one of the TW structures with attached mode launchers during measurement of the field profile (beadpull test).

Standing Wave Structures

For the single cell SW setup we used the dimensions of the NLC prototype SW structure SW20a565, with π phase advance per cell [3]. The SW20a565 cell dimensions are: cell radius 1.150 mm, cell length 11.312 mm, iris radius 5.65 mm, iris thickness 4.6 mm, major-axis of the elliptical iris tip 3.4 mm. In the single-cell SW structure, the cell radius was slightly modified to achieve the desired field profile.

We added two cells to the structure to create π-like fields in the test cell: a *matching cell* connected to circular waveguide and an *end cell* with a vacuum viewport. The geome-
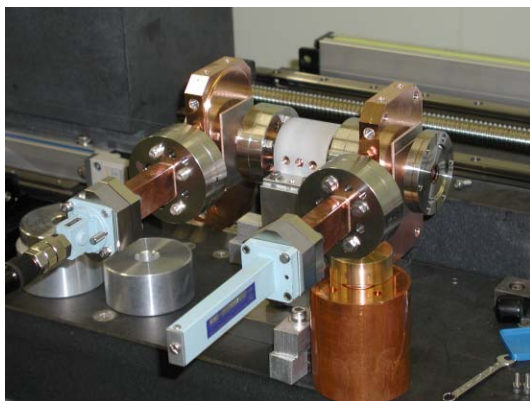
Figure 4: Single cell TW structure installed for bead-pull test.

tries of these two cells were chosen such that the structure is matched at the working frequency (critical coupling) and the maximum fields in these cells are half as large as the fields in the test cell.

The structure was designed with the 2D finite element code SLANS [7]. During the matching, four parameters were adjusted: the radii of all cells and the iris radius of the matching cell. The cell radii determine the field profile in the structure, and the iris of the matching cell determines the coupling of the structure to the circular waveguide. Afterward, the matching the solution was verified with the commercial electrodynamic code HFSS [8]. The field distribution in a copper single cell SW structure is shown in Fig. 5. We note that the same design procedure could be applied to structures with more than one cell for future study of the effect of the number of cell on breakdown behavior.
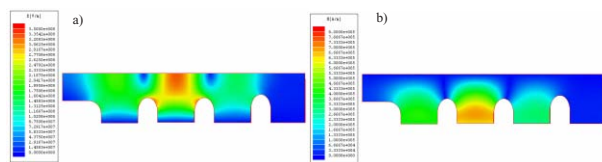

Figure 5: Amplitude of electric (a) and magnetic (b) fields in single cell copper SW structure for 10 MW of input power. The structure fed from the right, on the left, there is an opening with vacuum viewport.

We made two designs, one for testing of copper structure and another one for molybdenum. Since the resistivity of molybdenum is higher than that of copper, we changed the radii of all cells and radius of the matching iris of the molybdenum structure in order to maintain the field profile and critical coupling.

To date, a total of two copper SW structures have been built and successfully cold tested.

EXPERIMENTS

Different Materials

With copper TW and SW structures, we plan to study the effect of cell shape, circuit (SW *vs.* TW), and surface preparation methods on breakdown behavior. In addition, we have built a TW structure with iris tips made of molybdenum, and are building a TW and a SW structure made of solid molybdenum. We are going to compare breakdown limits and the conditioning behavior of these structures and the copper structures.

The structure shapes (for both SW and TW structures) and rf parameters, such as power and pulse width, for the these experiments will be close to those of practical structures. The importance of the choice of rf parameters was shown in experiments with CERN molybdenum TW structures, where short-pulse breakdown limit was higher than for copper. A similar structure operated at long-pulse length did not reach the copper breakdown limit [9].

Surface Processing

We are going to study the effect of different surface processing on breakdown behavior. We will use copper TW and SW structures for this experiment. We are going to compare standard SLAC/KEK processing of high gradient structures, high pressure water rinsing, and light etching of the assembled structure. The standard procedure includes etching of the structure cells only before bonding. All the structures will be assembled in a clean room and vacuum baked at 600° C for several days.

REFERENCES

[1] C. Adolphsen, "Normal Conducting RF Structure Test Facilities and Results," ROPC006, PAC03, Portland, Oregon, May 12-16, 2003.

[2] J. Wang and T. Higo, "Accelerator structure development for NLC / GLC," ICFA Beam Dyn. Newslett. **32**, 27 (2003).

[3] V. A. Dolgashev *et al*, "Status of X-band Standing Wave Structure Studies at SLAC," TPAB031, PAC03, Portland, Oregon, May 12-16, 2003.

[4] J.W. Wang, "RF Properties of Periodic Accelerating Structures for Linear Colliders," SLAC-Report-339, Ph.D. Dissertation, Stanford University, 1989.

[5] V.A. Dolgashev, S.G. Tantawi, "Simulations of Currents in X-band accelerator structures using 2D and 3D particle-in-cell code," FPAH057, PAC 2001, June 18-22, Chicago, Illinois. pp. 3807-3809.

[6] C. Nantista, S. Tantawi and V.A. Dolgashev, "Low-field accelerator structure couplers and design techniques," Phys. Rev. ST Accel. Beams 7, 072001 (2004), 7 pages.

[7] D. G. Myakishev *et al.* "An interactive code SLANS for evaluation of RF-cavities and accelerator structures," Proceedings of IEEE PAC01, 1991, San Francisco, Ca, pp.3002-3004.

[8] http://www.ansoft.com/products/hf/hfss/

[9] W. Wuensch *et al.*, "A High-Power Test of an X-Band Molybdenum-Iris Structure," THP34, this conference.